UDC 553.077
IRSTI 38.35.01

https://doi.org/10.55452/1998-6688-2026-23-2-464-480

[1]*Nygmanova A.S.,
MSc, Senior-lecturer, ORCID ID: 0009-0003-3917-2707,
e-mail: a.emls@kbtu.kz
[1]Korobkin V.V.,
Candidate of Geological and Mineralogical Sciences, Professor,
ORCID ID: 0000-0002-1562-759X, e-mail: korobkin_vv@kbtu.kz
[2]Buslov M.M.,
Doctor of Geological and Mineralogical Sciences, Professor, ORCID ID: 0000-0003-0606-2264,
e-mail: buslov@igm.nsc.ru
[1]Chaklikov A.Ye.,
PhD, Assistant Professor, ORCID ID: 0000-0001-8316-6599,
e-mail: a.chaklikov@kbtu.kz
[1]Tulemissova Zh.S.,
PhD, Associate Professor, ORCID ID: 0000-0003-1803-4535,
e-mail: z.tulemissova@kbtu.kz
[1,3]Koishibayev S.M.,
Master student, Consultant geologist, ORCID ID: 0009-0005-6492-4215
e-mail: skoishibayev@srk.kz

[1,3]Kazakh-British Technical University, Almaty, Kazakhstan
[2]Sobolev Institute of Geology and Mineralogy, Siberian Branch of the Russian Academy of Sciences, Novosibirsk State University, Novosibirsk, Russia
[3]SRK Consulting, Almaty, Kazakhstan

GEOLOGICAL AND MINERALOGICAL CONTROLS ON IRON SKARN FORMATION IN THE NORTHWESTERN BALKHASH REGION (CENTRAL KAZAKHSTAN)

Abstract

A comprehensive study has identified the principal geological and mineralogical controls governing the formation of iron skarn deposits in the Northwestern Balkhash region, based on representative deposits such as Zhuantobe and Karaulken. Integrated analysis of geological mapping, mineralogical and petrographic observations, geochemical data, and geophysical interpretations demonstrates that skarn formation represents a multistage contact-metasomatic system controlled by magmatic, structural, and fluid-related factors. Systematic patterns in the distribution of mineral assemblages and ore textural-structural types have been established, reflecting variations in fluid regimes and physicochemical conditions of ore formation. The obtained results refine the regional genetic model of iron skarn formation in the Northwestern Balkhash region and can be applied to the prediction and evaluation of the exploration potential of new ore targets.

Keywords: skarn deposits, magnetite ores, contact metasomatism, mineralogy, geophysical anomalies, Northwestern Balkhash region.

Received February 3, 2026; revised April 13, 2026; accepted April 30, 2026.

Introduction

Iron skarn deposits represent one of the most widespread and economically significant genetic types of iron mineralization. They typically form in contact zones between intrusive magmatic

bodies and carbonate or carbonate–siliceous sequences as a result of intensive contact metasomatic processes [1–8, 29]. Iron skarns are characterized by complex mineral assemblages, pronounced zoning, and high variability of textural and structural features, reflecting the multistage nature of ore formation [9–12].

The economic significance of iron skarn deposits is controlled not only by the total iron grade but also by the mode of iron occurrence, the crystallinity of magnetite, its relationships with rock-forming minerals, and the extent of retrograde and oxidative alterations [12–14]. These factors directly influence the technological properties of ores and their beneficiation efficiency, particularly during magnetic separation processes [10–14, 17–19].

Central Kazakhstan occupies a distinctive position among the iron ore provinces of Eurasia due to its complex tectono-magmatic evolution and the wide distribution of diverse iron ore deposit types [15–20]. Within this region, the Northwestern Balkhash area is of particular interest, hosting a cluster of iron skarn deposits and occurrences spatially associated with contact zones between Devonian carbonate–siliceous sequences and intermediate to felsic intrusive bodies.

Among the most studied and representative deposits in this area are Zhuantobe and Karaulken. These deposits are characterized by well-developed skarn mineralization, the presence of economically viable magnetite ores, and a pronounced structural control on mineralization [15–20]. At the same time, they exhibit differences in the degree of tectonic overprinting, mineralogical composition of skarns, and the nature of fluid–metasomatic evolution, making them suitable as representative case studies for identifying both general and site-specific patterns of iron skarn formation in the region.

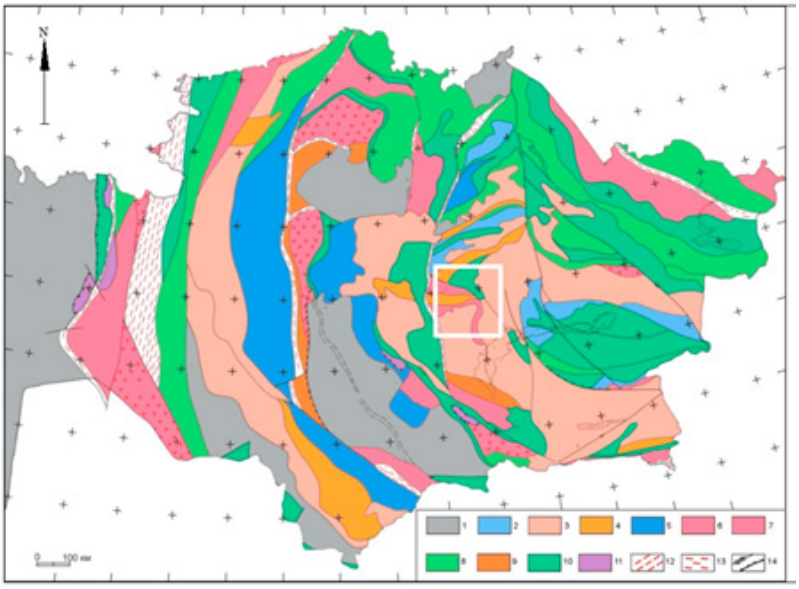

Figure 1 – Tectonic zoning scheme of the Paleozoic regions of Kazakhstan [6] (the iron ore district of the northwestern Balkhash area is highlighted by a white rectangle). The legend identifies 14 tectonic units: (1) Tectonic depressions, (2) Fragments of forearc terraces, (3) Volcanic and volcano–plutonic belts, (4) Rifts, (5) Folded strike–slip–thrust zones, (6) Cratonic terranes subject to weak granitization, (7) Cratonic terranes with granite–gneiss domes, (8) Fragments of volcanic island arcs, (9) Fragments of riftogenic basins, (10) Collisional sutures, (11) Ophiolitic allochthons, (12) Zones of transform sutures and suture zones, (13) Schist zones, (14) Collisional and post-collisional faults.

The aim of this study is to identify the geological and mineralogical characteristics of iron skarn formation in the Northwestern Balkhash region based on an integrated analysis of data from the Zhuantobe and Karaulken deposits, and to refine the regional genetic model of skarn mineralization.

Materials and methods

The study of the geological and mineralogical features of iron skarn formation in the Northwestern Balkhash region was carried out using an integrated set of field, laboratory, and analytical methods. The primary objects of investigation were the Zhuantobe and Karaulken iron skarn deposits, considered representative examples of regional skarn mineralization.

Field investigations included route-based geological and structural observations, detailed mapping of contact zones between intrusive bodies and carbonate–siliceous sequences, and examination of skarn alteration and ore mineralization. Particular attention was given to the identification of fault structures, fracture zones, and mylonitized zones controlling the spatial distribution of skarns and magnetite ore bodies.

Sampling was conducted from both outcrops and drill core obtained from exploration boreholes within ore-bearing zones. Sample collection was performed with consideration of lithological boundaries, the nature of metasomatic alterations, and textural–structural characteristics of the rocks. Sample lengths ranged from 0.15 to 2.7 m, with an average of approximately 1.5–1.7 m, ensuring the representativeness of the analytical dataset.

Mineralogical and petrographic studies were carried out using thin and polished sections. Transmitted-light microscopy of thin sections was performed using polarizing microscopes under plane-polarized and cross-polarized light conditions. This enabled the determination of mineral composition, identification of paragenetic assemblages, characterization of textural and structural features, and reconstruction of the sequence of metasomatic transformations.

Polished sections were examined in reflected light to study ore minerals. The analysis focused on the morphology of magnetite grains, their relationships with silicate minerals, the degree of martitization, and the distribution of sulfide phases. These observations were used to interpret the stages of ore formation and the conditions of magnetite crystallization.

To refine microtextural features and mineral morphology, scanning electron microscopy (SEM) coupled with energy-dispersive spectroscopy (EDS) was applied. Analyses were performed on polished sections at an accelerating voltage of approximately 20–25 kV. SEM–EDS observations allowed the identification of fine-scale textural features of magnetite, evidence of recrystallization and replacement processes, as well as the composition of microinclusions and secondary minerals.

The bulk chemical composition of rocks and ores was determined using X-ray fluorescence (XRF) analysis. Sample preparation included crushing, grinding, and pelletizing powdered material with binding agents; in some cases, glass fusion techniques were applied to improve sample homogeneity.

The analytical program included the determination of major oxides, primarily Fe_2O_3, SiO_2, CaO, Al_2O_3, and MgO, as well as trace and accessory components, including P_2O_5. Quality control of analytical data was ensured through duplicate measurements and comparison with certified reference materials. The obtained results were used to evaluate the chemical heterogeneity of skarns and to identify geochemical characteristics of magnetite ores.

Magnetic survey data were used to analyze the localization of iron skarn bodies. Interpretation of magnetic anomalies was carried out in conjunction with geological maps, cross-sections, and drilling data. Particular attention was given to the correlation between positive magnetic anomalies and zones of magnetite skarn development, which enabled refinement of the spatial distribution of ore bodies and their potential depth continuity.

Data processing was performed using an integrated approach combining geological, mineralogical, geophysical, and geochemical datasets. Interpretation was based on paragenetic analysis and the concept of multistage contact metasomatic ore formation. This approach allowed reconstruction of the sequence of iron skarn development and identification of the key factors controlling magnetite mineralization in the Northwestern Balkhash region.

Results

Geological Setting and Tectonic Framework of the Northwestern Balkhash Region

The Northwestern Balkhash region is located within the western segment of the Balkhash volcanic–plutonic belt, which forms part of the Central Asian Orogenic Belt (CAOB). The geological architecture of the region developed as a result of prolonged Paleozoic tectono-magmatic evolution, including stages of subduction, accretion, and subsequent collisional processes [20, 21].

The regional stratigraphic succession is dominated by Silurian–Devonian terrigenous–siliceous and carbonate sequences, represented by limestones, dolomites, siliceous shales, sandstones, and siltstones [10–17]. Carbonate units play a key role in the formation of iron skarns, acting as chemically reactive host rocks for interaction with magmatic and hydrothermal fluids.

Intrusive complexes in the region are represented by diorites, quartz diorites, granodiorites, and granites emplaced along deep-seated fault zones. These intrusions served as sources of heat and metal-bearing fluids and played a fundamental role in driving contact metamorphism and metasomatic processes.

The tectonic framework of the Northwestern Balkhash region is characterized by the development of strike-slip, thrust, and composite fault systems with northwestern, sublatitudinal, and meridional orientations [20]. These structures exerted a primary control on both the emplacement of intrusive bodies and the localization of skarn formation and ore accumulation.

Intersections of faults of different orders created zones of enhanced permeability, which facilitated the concentration of fluid flow and promoted the formation of magnetite ore bodies [18–20].

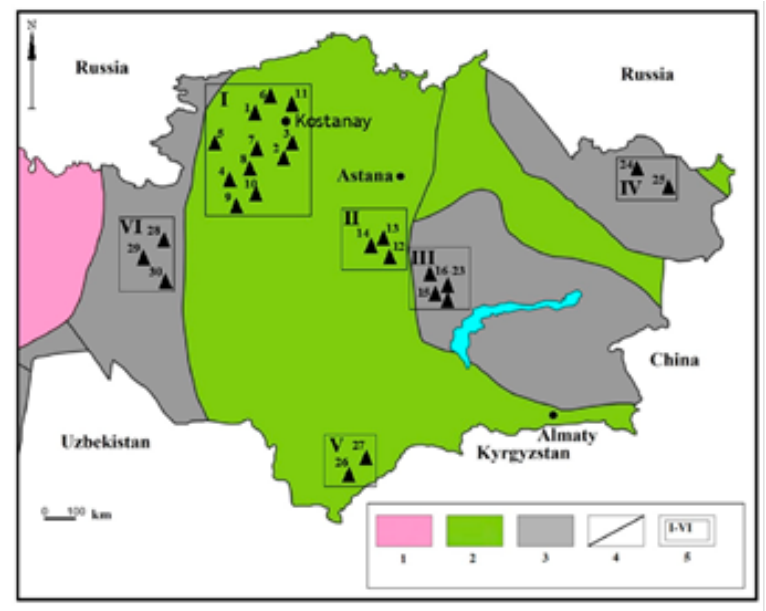

Figure 2 – Scheme of the main tectonic units and distribution of major industrial types of iron ore deposits in Kazakhstan: (1) East European Craton; (2, 3) Kazakh segment of the Central Asian Fold Belt: (2) Caledonian fold systems, (3) Hercynian fold systems; (4) geological boundaries; (5) outlines of iron ore districts. The deposits are grouped into six regions: I – Northern Torgay: 1. Kachar, 2. Sarbai, 3. Sokolov, 4. Lisakov, 5. Ayat, 6. Aleshino, 7. Lomonosov, 8. South Sarbai, 9. Sor, 10. Shagyrkol, 11. Korzhynkol; II – Central Kazakhstan: 12. Karazhal, 13. Ushkatyn, 14. Bolshoi Ktai; III – Northwestern Balkhash Region: 15. Bapy, 16. Zhuantobe, 17. Karaulken, 18. Akchagyl, 19. Ushtobe, 20. Kiyik, 21. Taitobe, 22. Tomashev, 23. Kyzyl-Sayak; IV – Eastern Kazakhstan: 24. Kholzun, 25. Rodionov Log; V – Southern Kazakhstan: 26. Irissu, 27. Abail; VI – Western Kazakhstan: 28. Velikhovskoye, 29. Kokbulak, 30. Taldy-Espe. III marks the position of the North Balkhash ore region, which hosts the Zhuantobe deposit

Geological Characteristics of Iron Skarn Deposits (Zhuantobe and Karaulken Case Studies)

The Zhuantobe iron skarn deposit is located in the central part of the Bapin ore field and is spatially associated with the contact zone between Silurian–Devonian carbonate and terrigenous–siliceous rocks and intrusive bodies of the granitoid complex. The geological structure of the deposit is complicated by a system of northwest-trending faults, which exert a primary control on the distribution of ore bodies [18–20].

Skarns at Zhuantobe are predominantly developed in exocontact zones and are represented by calcic–magnesian varieties dominated by pyroxene–garnet assemblages. Magnetite ore bodies occur as lenticular and stratiform bodies, characterized by significant thickness variability and frequently confined to zones of intense fracturing and brecciation. A distinctive feature of the Zhuantobe deposit is the widespread occurrence of massive and disseminated magnetite textures, reflecting intensive iron metasomatism. Near-surface zones are affected by oxidation processes, resulting in the formation of hematite and limonite.

The Karaulken deposit is located within the Akbastau fault zone and exhibits a more complex structural framework. The host rocks consist of Devonian carbonate–siliceous sequences intruded by diorite and diorite-porphyry bodies. Skarns are developed in both exocontact and endocontact zones. Karaulken is characterized by a more extensive development of retrograde skarns, represented by epidote–calcite and amphibole assemblages. Magnetite mineralization displays pronounced textural heterogeneity, including vein-type, brecciated, and crystallization-schistose ore varieties.

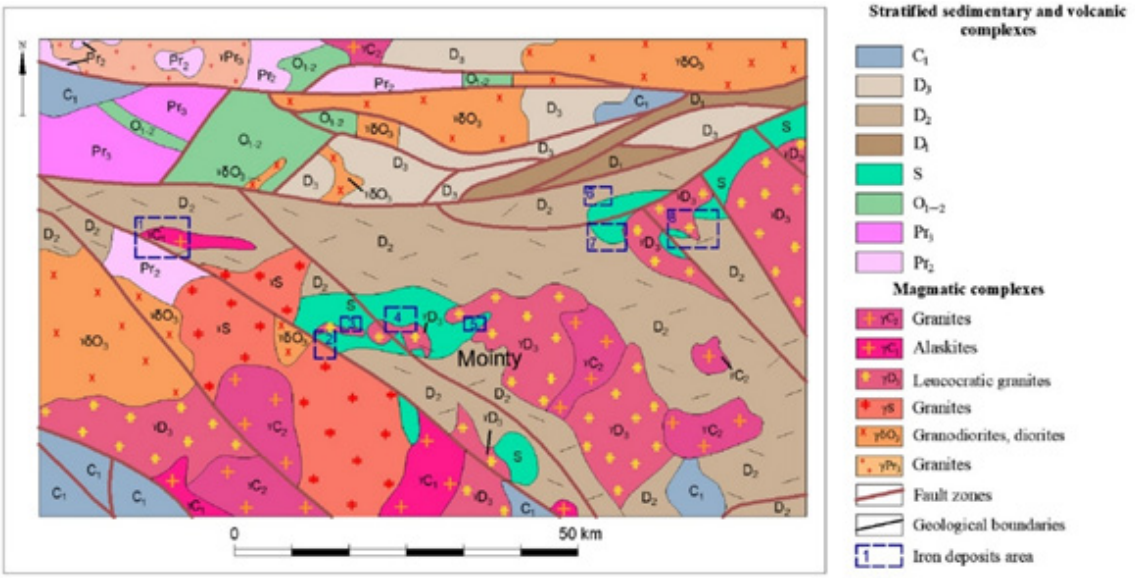

Figure 3 – The scheme of the geological structure of the iron ore region of the North-West Balkhash, compiled according to data [12, 14, 22]. The deposits are marked with blue contours:
(1) Kiyik, (2) Western Bapy, (3) Bapy, (4) Eastern Bapy, (5) Bale, (6) Ushtobe, (7) Akchagyl, (8) Zhuantobe

Geophysical Indicators of Iron Skarn Localization

Magnetic surveying represents one of the most informative methods for detecting iron skarn ore bodies in the Northwestern Balkhash region. Magnetite-bearing ores generate positive magnetic anomalies, the intensity and geometry of which are directly related to the thickness, morphology, and spatial distribution of ore bodies.

At the Zhuantobe deposit, high-amplitude magnetic anomalies are recorded, indicating the presence of massive magnetite accumulations and enabling the prediction of their depth continuity. In contrast, the Karaulken deposit exhibits a more complex magnetic field pattern, reflecting its block-faulted structural framework and the heterogeneous distribution of magnetite mineralization.

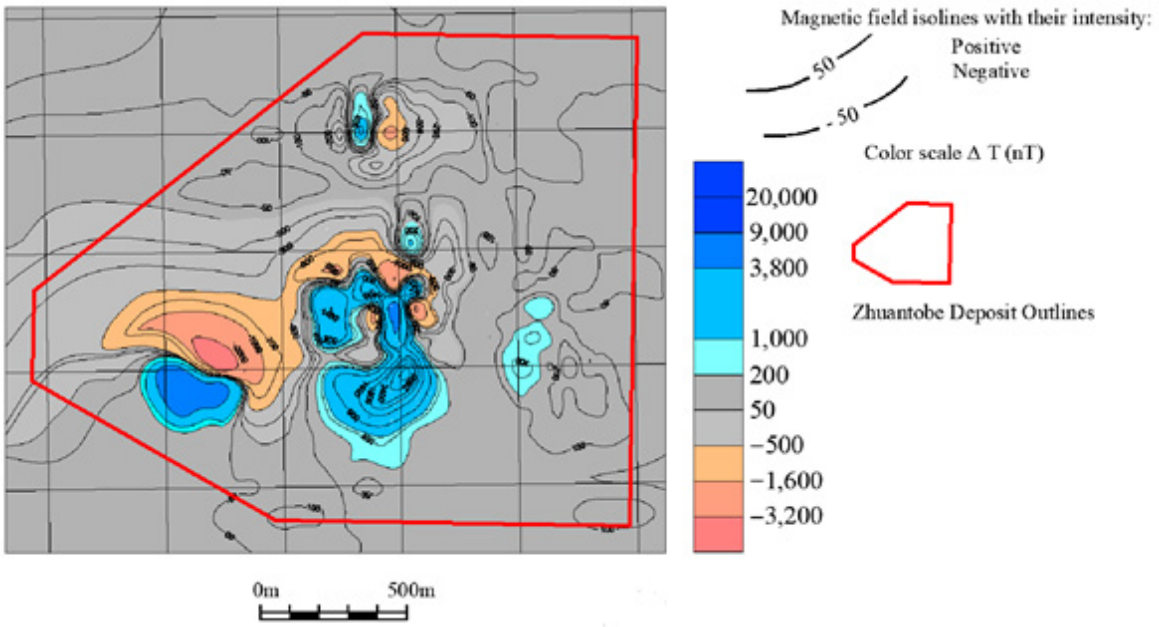

Figure 4 – Map of the magnetic field of the Zhuantobe deposit. Positive anomalies correspond to ore-bearing skarn zones. The map was compiled using field investigation results and supplemented with data from geophysical surveys [14, 22]

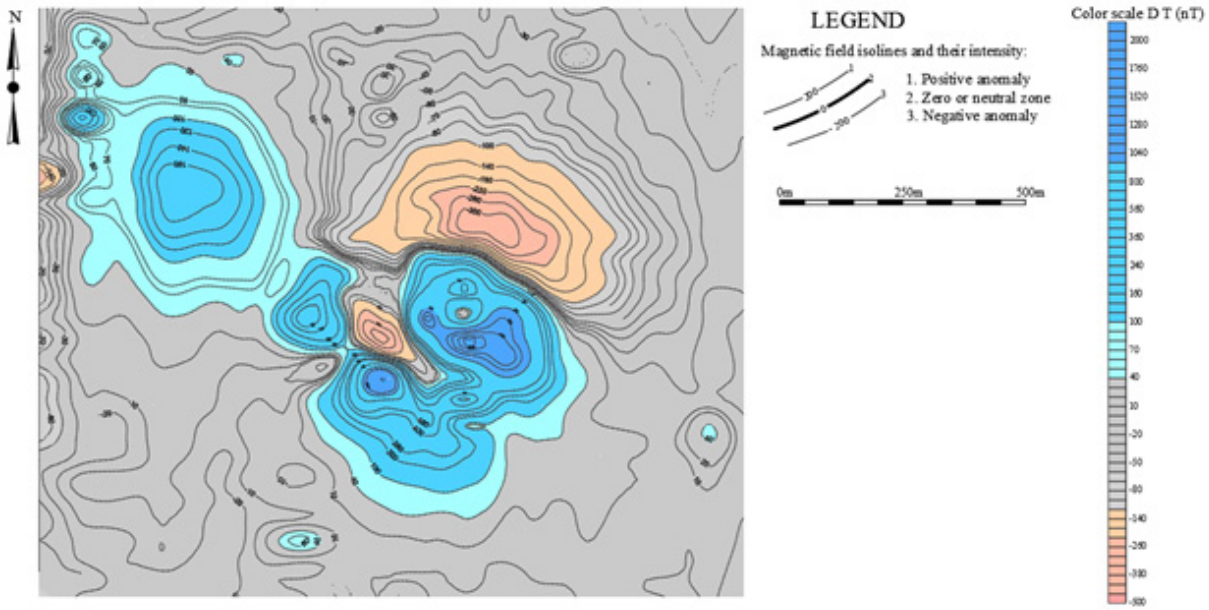

Figure 5 – Magnetic field map of the Karaulken deposit. Positive anomalies correspond to skarn ore-bearing zones. The map is based on field survey results and supplemented by geophysical data from [14, 22]

Mineralogical–Petrographic Characteristics and Composition of Skarns

Iron skarn formations of the Northwestern Balkhash region are characterized by considerable variability in mineral assemblages, textural–structural features, and degrees of metasomatic alteration of host rocks. Mineralogical and petrographic studies indicate that skarn assemblages at

the Zhuantobe and Karaulken deposits range from weakly altered marbles and hornfels to intensely metasomatized magnetite-bearing skarns and skarnoids.

The principal rock-forming minerals of the skarns include pyroxenes, garnets, epidote-group minerals, amphiboles, and calcite. Their relative abundance and morphological characteristics vary depending on the position within the contact zone, the intensity of fluid influence, and the stage of metasomatic evolution.

Pyroxenes are predominantly represented by diopside and, less commonly, hedenbergite. They occur as euhedral to subhedral crystals as well as aggregates of prismatic grains forming massive to weakly foliated textures. Pyroxenes are characteristic of the early anhydrous skarn stage and are widely developed in prograde skarns, particularly within exocontact zones.

Garnets are mainly represented by andradite and its solid-solution varieties, forming granular and porphyroblastic aggregates. They commonly contain inclusions of magnetite, epidote, and relic silicate minerals, indicating crystallization under conditions of intense iron metasomatism. Garnet-dominated skarns are especially characteristic of the Zhuantobe deposit, where they are closely associated with massive magnetite mineralization.

Epidote and epidote-group minerals are широко developed in retrograde skarns and skarnoids. They form fine-grained aggregates, veinlets, and replacement textures after pyroxenes and garnets. The occurrence of epidote reflects decreasing temperatures and an increasing role of aqueous fluids during the late stages of metasomatic evolution.

Amphiboles are represented mainly by hornblende and actinolite. They occur as prismatic crystals and fibrous aggregates replacing earlier pyroxenes. Amphiboles are particularly abundant in the Karaulken skarns, reflecting a more pronounced retrograde overprint.

Calcite is one of the dominant minerals of the late-stage assemblage and is widely distributed both within skarns and in vein and veinlet systems. It fills fractures, pores, and brecciated zones, forming mosaic and vein-type textures.

Magnetite is the principal ore mineral of the Northwestern Balkhash skarns. It occurs as massive accumulations, disseminated grains, veinlets, and brecciated aggregates. The morphology of magnetite ranges from equigranular and subhedral crystals to complex interstitial and vein-controlled forms, reflecting the dynamics of fluid flow and evolving physicochemical conditions. In near-surface zones, magnetite is partially replaced by hematite and limonite, forming martitized and limonitized ore varieties.

Sulfide minerals are represented predominantly by pyrite and, less commonly, chalcopyrite. They occur as fine disseminations, veinlets, and microinclusions within magnetite and the silicate matrix. Sulfide mineralization is mainly associated with the late hydrothermal stage and is subordinate relative to magnetite mineralization.

Mineralogical and petrographic data allow the identification of several successive stages of skarn formation:

1. Contact metamorphic stage, characterized by the formation of hornfels and marbles;
2. Prograde anhydrous skarn stage, marked by the development of pyroxene–garnet assemblages and primary magnetite;
3. Retrograde hydrothermal stage, accompanied by the formation of amphiboles, epidote, calcite, and sulfides;
4. Supergene oxidation stage, resulting in the replacement of magnetite by hematite and limonite.

Textural–Structural Features of Iron Skarns

Textural and structural characteristics of iron skarns in the Northwestern Balkhash region represent key indicators of their formation conditions and reflect the multistage evolution of contact metasomatic processes. Analysis of skarn textures and structures from the Zhuantobe and Karaulken deposits allowed the identification of several characteristic types, the formation of which is controlled by variations in thermodynamic conditions, fluid regimes, and tectonic activity.

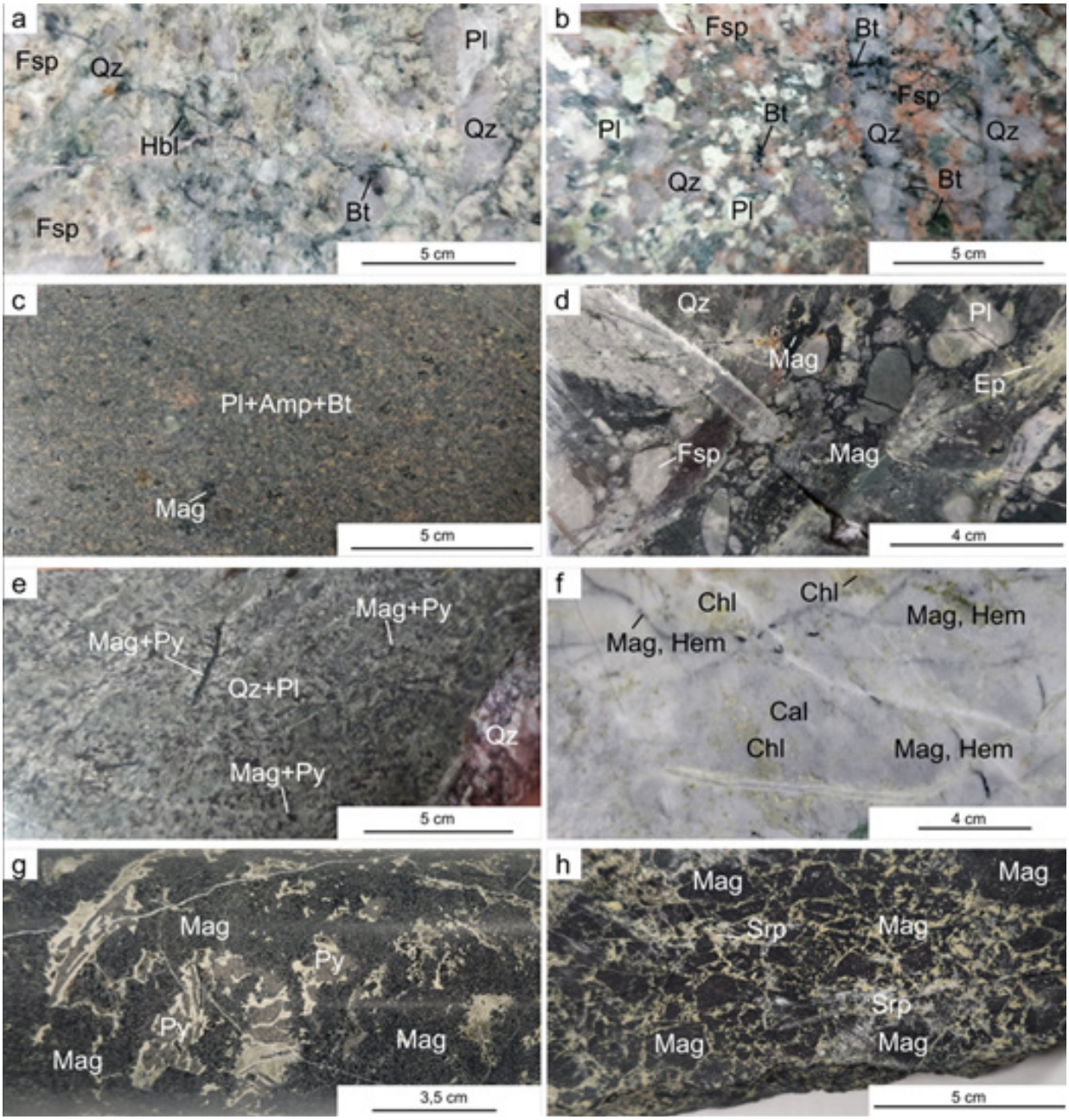

Figure 6 – Samples of the main rock types of the Zhuantobe deposit, details of Figure 5.
(a) Cataclastic coarse-grained granites, well Z01, from the depth 150.8 m; (b) silicified coarse-grained granites, well Z02, from the depth 142.0 m; (c) diorites, well Z01, from the depth 216.2 m; (d) cataclastic lithoclastic rhyolite tuffs, well Z02, from the depth 47.7; (e) skarns on sandstone, well Z04, from the depth 48.6 m; (f) marbles, well Z03, from the depth 121.7 m; (g) magnetite ores, well Z04, from the depth 40.1 m; (h) magnetite ores, well Z02, from the depth 150.2 m. Conventional indices of minerals [32]: feldspar (Fsp); quartz (Qz); hornblende (Hbl); biotite (Bt); plagioclase (Pl); amphibole (Amp); magnetite (Mag); epidote group minerals (Ep); pyrite (Py); chlorite (Chl); calcite (Cal); hematite (Hem); serpentine (Srp)

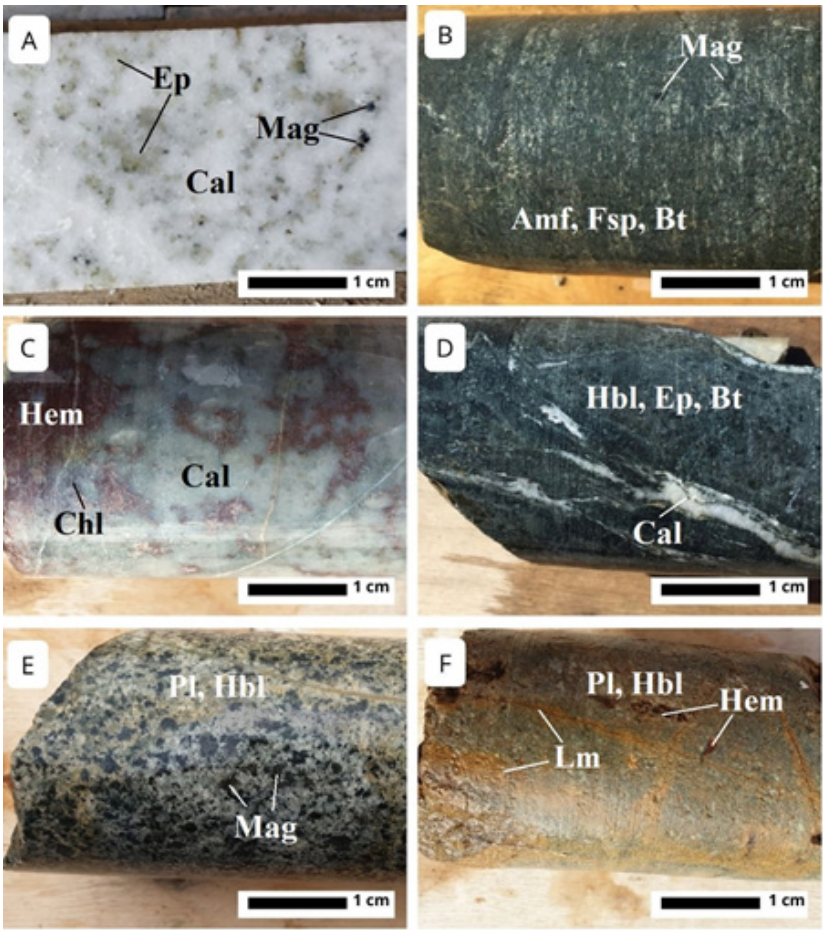

Figure 7 – Representative rock types of the Karaulken iron-skarn system (Central Kazakhstan). (A) Saccharoidal calcite marble with disseminated diopside–epidote grains from the contact zone; (B) Amphibolite from the prograde metamorphic zone; (C) Epidote–calcite skarn from the retrograde hydrothermal; (D) Actinolite–quartz–chlorite skarnoid from the transitional zone between prograde and retrograde stages; (E) Diorite from the intrusive complex; (F) Limonite–hematite skarnoid from the oxidation zone. Conventional indices of minerals (Whitney and Evans, 2010): epidote group minerals (Ep); magnetite (Mag); calcite (Cal); amphibole (Amp); feldspar (Fsp); biotite (Bt); hematite (Hem); chlorite (Chl); hornblend (Hbl); plagioclase (Pl); limonite (Lm)

Massive textures are typical of zones of intense iron metasomatism and are represented by dense accumulations of magnetite with a minor proportion of silicate matrix. Magnetite forms equigranular to subhedral crystals tightly intergrown, giving the ores a compact, monolithic appearance. These textures develop under conditions of high Fe-rich fluid activity and relatively stable thermal regimes.

Disseminated textures are characterized by an uneven distribution of magnetite within a silicate skarn matrix. Ore minerals occur as isolated grains or small aggregates interstitially distributed among pyroxene, garnet, epidote, and amphibole. Grain size varies from microscopic to millimeter scale. These textures reflect less intensive iron metasomatism and indicate conditions where ore formation occurred contemporaneously with the growth of silicate minerals. Disseminated textures are widely developed at both Zhuantobe and Karaulken and are typical of transitional zones between ore-bearing and barren skarns.

Vein and veinlet textures are represented by networks of magnetite, quartz–calcite, and epidote–calcite veinlets crosscutting the skarn matrix. Magnetite within these structures forms elongated

aggregates commonly aligned along fractures and zones of tectonic brecciation. Vein–disseminated textures reflect a pulsatory fluid flow regime and repeated reactivation of fault structures. These textures are particularly characteristic of the Karaulken deposit, where ore zones are closely associated with strike-slip and thrust fault systems. Genetically, they are interpreted as products of late-stage skarn formation and the onset of hydrothermal overprinting.

Brecciated textures develop within zones of intense tectonic deformation and consist of angular to subrounded fragments of skarns and host rocks cemented by magnetite, calcite, epidote, and secondary silicates. The variability in fragment size and morphology indicates multiple episodes of fragmentation followed by mineral precipitation. The presence of brecciated textures highlights the significant role of tectonics in ore formation and indicates repeated reopening of the system for fluid circulation. These textures are especially characteristic of Karaulken and reflect a prolonged and complex deformation history.

Crystallization-schistose textures form under conditions of directed stress and ductile deformation. They are expressed by the preferred orientation of prismatic and tabular amphibole and epidote crystals, as well as elongated magnetite aggregates. Such textures develop during late stages of skarn evolution under the combined influence of tectonic deformation and hydrothermal processes.

In terms of structure, skarns range from coarse- and medium-grained to fine-grained and cryptocrystalline varieties. Coarse-grained structures are typical of early prograde skarns, whereas fine-grained and recrystallized textures reflect retrograde alteration and repeated fluid activity.

Magnetite ores commonly exhibit replacement, interstitial, and corrosion textures, indicating complex relationships between ore and rock-forming minerals. These features confirm the multistage nature of iron skarn formation in the Northwestern Balkhash region.

The integrated analysis of textural–structural features allows the interpretation of iron skarn formation as a result of a multistage evolutionary system involving:

- Prograde skarn formation under high-temperature conditions and intensive iron metasomatism;
- Subsequent hydrothermal overprinting, leading to the development of vein and brecciated textures;
- Tectonic reorganization of ore zones, resulting in oriented and schistose structures;
- Near-surface oxidation processes, causing secondary alteration of magnetite into hematite and limonite.

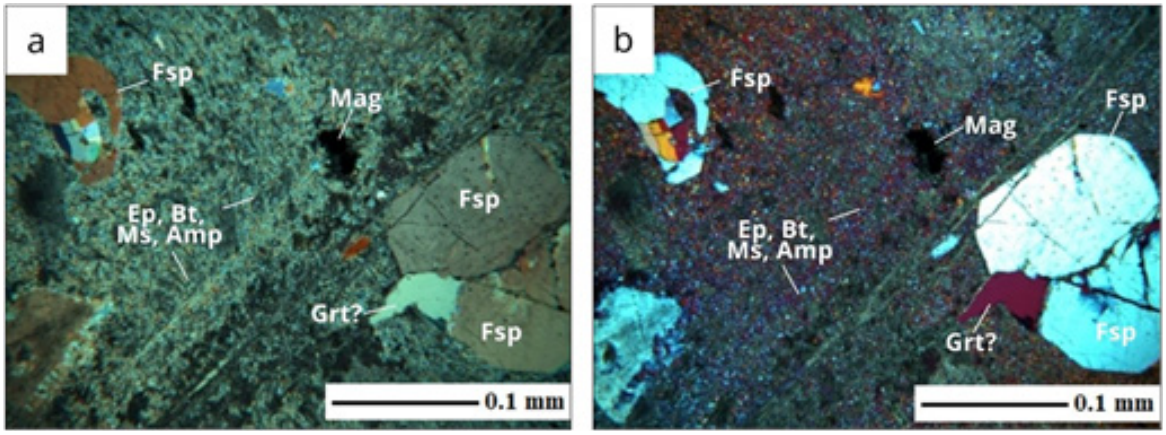

Figure 8 – Garnet–epidote skarns with magnetite from Zhuantobe deposit: (a) parallel nicols; (b) crossed nicols with compensator; magnification ×40. Conventional indices of minerals [32]: feldspar (Fsp); magnetite (Mag); epidote group minerals (Ep); biotite (Bt); muscovite (Ms); amphibole (Amp); probable garnet (Grt?)

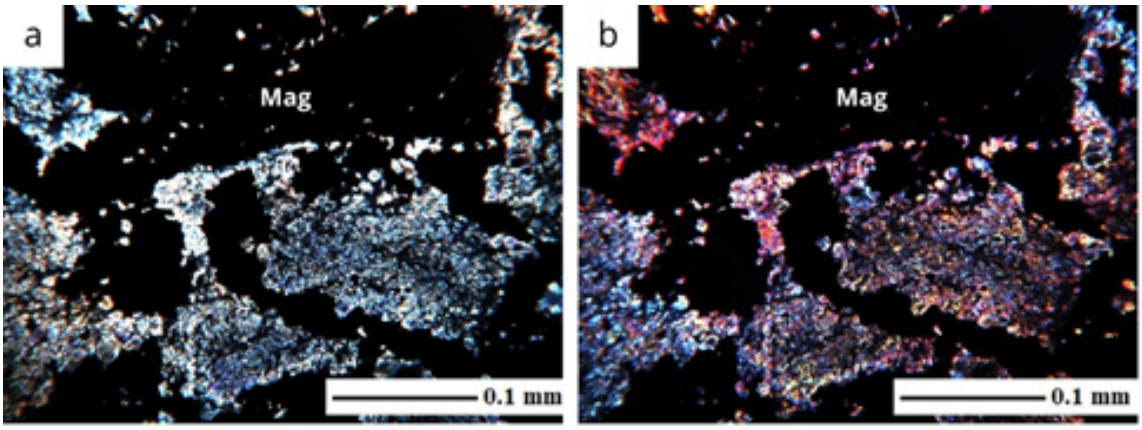

Figure 9 – Magnetite ores from Karaulken deposit: (a) parallel nicols;
(b) crossed nicols with compensator; magnification ×40. Conventional indices of minerals [32]:
magnetite (Mag).

Bulk Composition and Geochemical Characteristics of Iron Skarns

Geochemical data obtained from the Zhuantobe and Karaulken deposits provide key insights into the distribution patterns of iron and associated elements within skarn systems of the Northwestern Balkhash region.

The chemical composition of skarns is controlled by the interplay between the composition of carbonate–siliceous host rocks and the nature of magmatic–hydrothermal processes. Most skarn varieties are characterized by elevated contents of Fe_2O_3, CaO, and SiO_2, with variable concentrations of Al_2O_3, MgO, and MnO. This compositional pattern reflects intensive silicification and iron metasomatism associated with the formation of magnetite mineralization.

Bulk Composition and Geochemical Characteristics of Iron Skarns

Geochemical data obtained from the Zhuantobe and Karaulken deposits provide key insights into the distribution patterns of iron and associated elements within skarn systems of the Northwestern Balkhash region.

The chemical composition of skarns is controlled by the interplay between the composition of carbonate–siliceous host rocks and the nature of magmatic–hydrothermal processes. Most skarn varieties are characterized by elevated contents of Fe_2O_3, CaO, and SiO_2, with variable concentrations of Al_2O_3, MgO, and MnO. This compositional pattern reflects intensive silicification and iron metasomatism associated with the formation of magnetite mineralization.

Fe_2O_3 contents in skarns and ores vary widely, ranging from moderate values in weakly altered rocks to high concentrations in massive magnetite bodies. Maximum values are typical of prograde skarns, where iron is predominantly concentrated in magnetite. In retrograde assemblages, iron is redistributed among magnetite, hematite, and iron hydroxides.

Calcium and silicon represent the principal components of the skarn matrix and are mainly incorporated into pyroxene, garnet, epidote, and calcite. The relative proportions of CaO and SiO_2 depend on the degree of replacement of carbonate rocks by silicate minerals and the intensity of subsequent hydrothermal alteration.

Ore bodies at Zhuantobe and Karaulken are dominated by magnetite as the principal iron-bearing phase. Geochemical data indicate that magnetite ores are characterized by relatively low silica contents and elevated iron concentrations, which positively influence their metallurgical properties.

At the Zhuantobe deposit, magnetite ores generally exhibit a more homogeneous chemical composition and relatively stable Fe_2O_3 contents. This is attributed to the predominance of massive and disseminated textures formed under conditions of sustained and intensive iron metasomatism. These ores are characterized by low concentrations of deleterious elements, making them favorable for beneficiation.

In contrast, Karaulken ores display pronounced geochemical heterogeneity, expressed by fluctuations in iron content, elevated SiO_2 concentrations, and local enrichment in P_2O_5. These features are related to a more complex structural setting, multi-stage reactivation of fault zones, and intense retrograde alteration of skarns.

Trace and associated elements in iron skarns are mainly represented by Mn, Ti, Al, and P, occurring in both ore and rock-forming minerals. Manganese commonly substitutes for iron in magnetite and pyroxenes, whereas titanium is present as fine inclusions of ilmenite or titanomagnetite.

Phosphorus is one of the most critical technological components affecting ore quality. Elevated P2O5 contents in certain zones of Karaulken are associated with the presence of apatite and secondary phosphate minerals formed during late hydrothermal stages. The heterogeneous distribution of P_2O_5 necessitates a differentiated approach to resource evaluation and processing strategies.

Sulfur contents are generally low and are associated with the presence of pyrite and, less commonly, chalcopyrite. Sulfide mineralization is subordinate and does not significantly affect the overall composition of the ores; however, its presence serves as an important indicator of late hydrothermal processes.

The analysis of bulk composition demonstrates that geochemical characteristics are closely linked to the stages of skarn system evolution. The prograde stage is marked by maximum iron concentration and the formation of relatively simple magnetite-dominated assemblages. During the retrograde stage, redistribution of components occurs, accompanied by enrichment in calcium and silicon and localized accumulation of trace elements.

The bulk composition of iron skarns directly influences their technological properties. The predominance of magnetite and relatively low levels of harmful impurities in Zhuantobe ores result in high beneficiation efficiency and the production of high-grade concentrates. In contrast, the more complex composition of Karaulken ores requires detailed mineralogical and technological evaluation and the application of combined processing methods.

Overall, the geochemical characteristics of iron skarns in the Northwestern Balkhash region reflect the complex evolution of contact metasomatic systems and provide a robust basis for genetic interpretations and practical applications in exploration and resource development.

Table 1 – Generalized bulk composition of iron skarns in the Northwestern Balkhash region (Zhuantobe and Karaulken)

Component	Content range, wt.%	Average, wt.%	Mineral host	Genetic interpretation
Fe_2O_3	25.0 – 55.0	38.0 – 42.0	Magnetite, hematite	The main ore component, the prograde stage of skarn formation
SiO_2	15.0 – 35.0	22.0 – 27.0	Pyroxenes, garnets, quartz	Silicate matrix of skarns, intensity of silicification
CaO	10.0 – 30.0	18.0 – 22.0	Calcite, garnets, epidote	Metasomatic substitution carbonate breeds
Al_2O_3	3.0 – 10.0	5.0 – 7.0	Garnets, epidote, amphiboles	The introduction of aluminum during magmatic -hydrothermal action
MgO	2.0 – 8.0	3.5 – 5.0	Pyroxenes, amphiboles	Calcium-magnesium type skarnov
MnO	0.1 – 1.5	0.3 – 0.7	Magnetite, pyroxenes	Isomorphic impurities in ore minerals
TiO_2	0.1 – 1.0	0.2 – 0.5	Ilmenite, titanomagnetite	Magmatic component ore-bearing fluids
P_2O_5	0.05 – 3.0	0.3 – 1.2	Apatite	Late hydrothermal processes, a technologically important component
SO_3	0.01 – 1.0	0.1 – 0.3	Pyrite, sulfates	Subordinate sulfide mineralization

Discussion

A comparative analysis of the geology, mineralogy, and formation conditions of iron skarns in the Northwestern Balkhash region with global analogues reveals both fundamental similarities and region-specific features. International studies demonstrate that iron skarn deposits represent significant sources of high-grade iron ores, typically formed at the contact between magmatic intrusions and carbonate sequences under the influence of magmatic–hydrothermal fluids [23, 27, 30–33]. Established genetic models emphasize multistage skarn evolution, including prograde and retrograde stages involving magnetite, pyroxene, garnet, and epidote assemblages.

For example, studies of the Zanjan iron skarn deposits (Iran) [23] indicate the development of both magnesian and calcic skarns (endoskarn and exoskarn), formed at the contact between granitic intrusions and carbonate rocks and characterized by pyroxene–garnet–magnetite associations. Similarly, investigations of the high-grade Jinling iron skarn deposit (North China) reveal well-defined mineralogical zoning and clear stage evolution, where early iron enrichment is associated with Fe-rich hydrothermal fluids, followed by retrograde mineralization and secondary silicate formation [30–33].

The comparative analysis indicates that iron skarns of the Northwestern Balkhash region conform to the principal characteristics of global iron skarn systems:

- spatial association with контакт zones between intermediate to felsic intrusions and carbonate sequences;
- multistage evolution involving prograde and retrograde phases;
- mineral assemblages dominated by magnetite, pyroxene, garnet, and epidote;
- strong structural control by fault systems facilitating fluid migration.

Despite this general genetic framework, several distinctive features of the Northwestern Balkhash skarns can be identified:

- more pronounced tectonic overprinting, expressed by the development of vein systems and brecciated structures, typical of the Central Asian Orogenic Belt;
- significant textural heterogeneity related to repeated reactivation of fault zones, comparable to skarn systems in the Tianshan–Beishan region;
- geochemical variability, including elevated concentrations of impurity elements (e.g., phosphorus), similar to patterns observed in North China skarns.

Global syntheses indicate that, although iron skarn deposits form under a wide range of geological conditions, they are unified by a common contact metasomatic mechanism driven by magmatic heat and fluid circulation. This framework is consistent with the genetic model proposed for the Northwestern Balkhash region, confirming its classification as a typical iron skarn system within an active continental margin–type geodynamic setting.

Conclusion

This study establishes the key geological and mineralogical patterns governing the formation of iron skarns in the Northwestern Balkhash region, based on detailed investigation of the Zhuantobe and Karaulken deposits. Integrated analysis of geological mapping, mineralogical–petrographic observations, geochemical data, and geophysical interpretation demonstrates that skarn formation represents a multistage contact metasomatic system controlled by magmatic, structural, and fluid-related factors.

Mineralogical and petrographic data confirm the multistage evolution of skarn assemblages. The prograde anhydrous stage is characterized by the formation of pyroxene–garnet assemblages and primary magnetite mineralization. During the retrograde stage, skarns undergo hydrothermal reworking accompanied by the development of amphiboles, epidote, calcite, and subordinate sulfide mineralization. Near-surface oxidation processes result in partial replacement of magnetite by hematite and limonite, leading to additional mineralogical and geochemical differentiation of ores.

Fault-block tectonics plays a fundamental role in controlling the emplacement of intrusions and the migration of ore-forming fluids, thereby governing the localization of mineralization. The more интенсив tectonic overprinting observed at Karaulken results in increased geochemical heterogeneity compared to the более stable conditions of ore formation at Zhuantobe.

Comparison with global iron skarn systems indicates that the Northwestern Balkhash deposits correspond to classical iron skarns associated with active continental margin environments and the Central Asian Orogenic Belt.

The identified geological, mineralogical, and geochemical criteria can be applied in the prediction and exploration of new iron ore targets, as well as in the assessment of technological properties of ores and the selection of optimal processing strategies for their industrial development.

REFERENCES

1 Satpayev, K.I. Main patterns of spatial distribution of endogenous mineralization zones in Central Kazakhstan. Soviet Geology, 58, 93–109 (1957). (in Russian).

2 Novokhatsky, I.P. Genetic types of iron ore deposits in Central Kazakhstan. In: Iron Ore Deposits of Central Kazakhstan and Ways of Their Use (Moscow: USSR Academy of Sciences, 1960). (in Russian).

3 Satpayev, K.I. Selected Works. Problems of Metallogeny and Mineral Resources of Kazakhstan, Vol. 3 (Alma-Ata: Nauka, 1968), 312 p. (in Russian).

4 Shcherba, G.N. Atasu type deposits in Kazakhstan. Endogenous Ore Deposits, pp. 185–196 (1968). (in Russian).

5 Bogdanov, A.A. Tectonic zoning of the Paleozoides of Central Kazakhstan and Tien Shan. Bulletin of the Moscow Society of Naturalists, 40, 8–42 (1965). (in Russian).

6 Bespalov, V.F. Tectonic Map of the Kazakh SSR and Adjacent Territories of the Union Republics at a Scale of 1:1,500,000. Explanatory Note (Alma-Ata, 1975), 160 p. (in Russian).

7 Dymkin, A.M. Contact-Metasomatic Iron Deposits of the Southern Part of the Main Ore Belt of Turgay (Novosibirsk: Publishing House of the Siberian Branch of the USSR Academy of Sciences, 1962), 239 p. (in Russian).

8 Esenov, Sh.E., Lyapichev, G.F., Sidorenko, A.V., and Shlygin, E.D. Geology of the USSR. Vol. XX. Central Kazakhstan. Geological Description. Book 1 (Moscow: Nedra, 1972), 532 p. (in Russian).

9 Zaicev, Yu.A. Geology of the USSR. Vol. XX. Central Kazakhstan. Minerals (Moscow: Nedra, 1979), 541 p. (in Russian).

10 Abdulin, A.A. Geology and Mineral Resources of Kazakhstan (Almaty: Gylym, 1994), 394 p. (in Russian).

11 Zholtayev, G.Zh., Zhukov, N.M., and Antonenko, A.A. Atlas of Solid Mineral Deposits of the Republic of Kazakhstan (Almaty: K.I. Satpayev Institute of Geological Sciences, 2024), 263 p. (in Russian).

12 Bekzhanov, G.R., Koshkin, V.Y., and Nikitchenko, I.I. Geological Structure of Kazakhstan (Almaty: AMR of the Republic of Kazakhstan, 2000), 396 p. (in Russian).

13 Bekmukhametov, A.E. Magmatogenic Iron Ore Formations (Moscow: Nedra, 1987), 212 p. (in Russian).

14 Kubeeva, L.V., Zyabkin, V.F., Yugay, V.D., Baimuldina, N.N., and Muzgina, V.S. Geoecological studies during the development of the Bapy iron ore deposit in the Republic of Kazakhstan. Subsoil Use in the 21st Century, 1, 81–83 (2010). (in Russian).

15 Bekmukhametov, A.E., Pankratova, N.L., and Kryukov, A.S. Iron Ore Formations. Chu-Ili Belt. Minerals (Alma-Ata: Nauka, 1980). (in Russian).

16 Zhukov, N.M., Akylbekov, S.A., Antonenko, A.A., and Amanbayev, R. Iron Deposits of Kazakhstan: A Handbook (Almaty, 2016), 258 p. (in Russian).

17 Daukeev, S.Zh., Uzhkenov, B.S., Abdulin, A.A., Bespaev, Kh.A., Votsalevsky, E.S., Lyubetsky, V.N., Mazurov, A.K., and Miroshnichenko, L.A. Deep Structure and Geodynamics. In: Deep Structure and Mineral Resources of Kazakhstan, Vol. 1 (Almaty: National Academy of Sciences of the Republic of Kazakhstan, 2002), 224 p. (in Russian).

18 Daukeev, S.Zh., Uzhkenov, B.S., Abdulin, A.A., Miroshnichenko, L.A., Zhukov, N.M., Mazurov, A.K., Bespaev, Kh.A., Dolgopolov, B.M., Akylbekov, S.A., Zhautikov, T.M., and Gubaidulin, F.G. Metallogeny. In: Deep Structure and Mineral Resources of Kazakhstan, Vol. 2 (Almaty: National Academy of Sciences of the Republic of Kazakhstan, 2002), 265 p. (in Russian).

19 Nikitchenko, I.I. Minerals of Kazakhstan: Explanatory Note to the Map of Minerals of Kazakhstan at a Scale of 1:1,000,000 (Kokshetau: Ministry of Energy and Mineral Resources of the Republic of Kazakhstan, 2002), 188 p. (in Russian).

20 Korobkin, V.V., and Buslov, M.M. Tectonics and geodynamics of the western Central Asian Fold Belt (Kazakhstan Paleozoides). Russian Geology and Geophysics, 52, 1600–1618 (2011). https://doi.org/10.1016/j.rgg.2011.11.011

21 Korobkin, V.V., Chaklikov, A.Y., and Tulemissova, Z.S. Tectonic zoning of Paleozoides of Kazakhstan and its oil and gas-bearing regions. Kazakhstan Journal for Oil & Gas Industry, 4(1), 39–49 (2022). https://doi.org/10.54859/kjogi107854

22 Boyko, O.N., Filatova, G.V., Zyabkin, V.F., and Lim, D.K. Report on the Results of Exploration of Iron-Containing Ores in the Bapy Area in the Karaganda Region for 2015–2018 (Karaganda, 2019).

23 Zhao, W.W., and Zhou, M.F. In-situ LA-ICP-MS trace elemental analyses of magnetite: The Mesozoic Tengtie skarn Fe deposit in the Nanling Range, South China. Ore Geology Reviews, 65(4), 867–883 (2015). https://doi.org/10.1016/j.oregeorev.2014.09.019

24 Korobkin, V., Chaklikov, A., Tulemissova, Z., Samatov, I., and Dobrovolskaya, Y. Results of the Study of Epigenetic Changes of Famennian–Tournaisian Carbonate Rocks of the Northern Marginal Shear Zone of the Caspian Syneclise (Kazakhstan). Minerals, 13, 249 (2023). https://doi.org/10.3390/min13020249

25 Korobkin, V., Samatov, I., Chaklikov, A., and Tulemissova, Z. Peculiarities of Dynamics of Hypergenic Mineral Transformation of Nickel Weathering Crusts of Ultramafic Rocks of the Kempirsay Group of Deposits in Western Kazakhstan. Minerals, 12, 650 (2022). https://doi.org/10.3390/min12050650

26 Korobkin, V.V., Tulemissova, Z.S., Samatov, I.B., and Chaklikov, A.Y. Secondary calcite in carbonate reservoirs of oil fields: a method for its quantitative determination. Kazakhstan Journal for Oil & Gas Industry, 7(2), 84–95 (2025). (in Russian). https://doi.org/10.54859/kjogi108822

27 Vezzoni, S., Rocchi, S., and Dini, A. Campiglia Marittima Skarn (Tuscany): A Challenging Example for the Evolution of Skarn-Forming Models. Minerals, 13, 482 (2023). https://doi.org/10.3390/min13040482

28 Vom Rath, G. Die Berge von Campiglia in der Toskanischen Maremme. Zeitschrift der Deutschen Geologischen Gesellschaft, 20, 307–364 (1868).

29 Reverdatto, V.V. Facies of Contact Metamorphism (Moscow: Nedra, 1970), 272 p. (in Russian).

30 Chen, Y., Cao, Y., Liu, L., Wang, C., Yang, W., Gai, Y., Xie, T., Song, L., and Xie, F. Elucidating the Genetic Mechanism and the Ore-Forming Materials of the Kaladawan Iron Deposit in the North Altyn Tagh, Western China. Minerals, 14, 589 (2024). https://doi.org/10.3390/min14060589

31 Yi, J., Shi, X., Ji, G., Zhang, L., Wang, S., and Deng, H. The Geochemical Characteristics of Trace Elements in Magnetite and Fe Isotope Geochemistry of the Makeng Iron Deposit in Southwest Fujian and Their Significance in Ore Genesis. Minerals, 14, 217 (2024). https://doi.org/10.3390/min14030217

32 Feng, Q., Gao, M., Fu, C., Li, S., Li, Y., Gao, J., Ma, M., Wang, Z., Zhu, Y., Wu, B., Duan, Z., and Dang, Z. Phlogopite 40Ar/39Ar Geochronology for Guodian Skarn Fe Deposit in Qihe–Yucheng District, Luxi Block, North China Craton: A Link between Craton Destruction and Fe Mineralization. Minerals, 14, 690 (2024). https://doi.org/10.3390/min14070690

33 Li, Y., Jiang, Z., Wang, D., Zhang, Z., and Duan, S. Genesis of the Beizhan Iron Deposit in Western Tianshan, China: Insights from Trace Element and Fe–O Isotope Compositions of Magnetite. Minerals, 14, 304 (2024). https://doi.org/10.3390/min14030304

34 Matiolo, E., Couto, H.J.B., Lima, N., Silva, K., and de Freitas, A.S. Improving recovery of iron using column flotation of iron ore slimes. Minerals Engineering, 158, 106608 (2020). https://doi.org/10.1016/j.mineng.2020.106608

35 Nakhaei, F., and Irannajad, M. Reagents types in flotation of iron oxide minerals: A review. Mineral Processing and Extractive Metallurgy Review, 39(2), 89–124 (2018). https://doi.org/10.1080/08827508.2017.1391245

36 Silva, R.C.F., Ardisson, J.D., Cotta, A.A.C., Araujo, M.H., and de Carvalho Teixeira, A.P. Use of iron mining tailings from dams for carbon nanotubes synthesis in fluidized bed for 17α-ethinylestradiol removal. Environmental Pollution, 260, 114099 (2020). https://doi.org/10.1016/j.envpol.2020.114099

37 Araujo, A.C., Amarante, S.C., Souza, C.C., and Silva, R.R.R. Ore mineralogy and its relevance for selection of concentration methods in processing of Brazilian iron ores. Mineral Processing and Extractive Metallurgy, 112(1), 54–64 (2003). https://doi.org/10.1179/037195503225011439

38 Lima, R.M.F., and Abreu, F.P.V.F. Characterization and concentration by selective flocculation/magnetic separation of iron ore slimes from a dam of Quadrilátero Ferrífero – Brazil. Journal of Materials Research and Technology, 9, 12356–12362 (2020). https://doi.org/10.1016/j.jmrt.2019.12.034

39 Muwanguzi, A.J.B., Karasev, A.V., Byaruhanga, J.K., and Jönsson, P.G. Characterization of the Physical and Metallurgical Properties of Natural Iron Ore for Iron Production. ISRN Materials Science, Article 147420 (2012). https://doi.org/10.5402/2012/147420

40 Yellishetty, M., Ranjith, P.G., and Tharumarajah, A. Iron ore and steel production trends and material flows in the world: Is this really sustainable? Resources, Conservation and Recycling, 54(12), 1084–1094 (2010). https://doi.org/10.1016/j.resconrec.2010.03.003

41 Zhang, X., Gu, X., Han, Y., Parra-Álvarez, N., Claremboux, V., and Kawatra, S.K. Flotation of Iron Ores: A Review. Mineral Processing and Extractive Metallurgy Review, 42(3), 184–212 (2021). https://doi.org/10.1080/08827508.2019.1689494

42 Ostadrahimi, M., Farrokhpay, S., Zare, T., Aghajanlou, M., Gharibi, K., and Salari Rad, M.M. An Integrated Separation Approach for Beneficiation of Low-Grade Iron Ore. Minerals, 15(9), 958 (2025). https://doi.org/10.3390/min15090958

43 Prasad, J., Venkatesh, A.S., Sahoo, P.R., Singh, S., and Sylvestre Kanouo, N. Geological Controls on High-Grade Iron Ores from Kiriburu-Meghahatuburu Iron Ore Deposit, Singhbhum-Orissa Craton, Eastern India. Minerals, 7(10), 197 (2017). https://doi.org/10.3390/min7100197

44 Mahanta, C.R., Sahoo, P.R., Mohanta, M.K., Rath, R.K., Dey, S., Tripathy, S.K., Prasad, J., and Venkatesh, A.S. Mineralogical Characteristics of Hematitic Iron Ore: A Geometallurgical Study on Ore from Eastern India. Minerals, 13(9), 1194 (2023). https://doi.org/10.3390/min13091194

45 Maniteja, M., Samanta, G., Gebretsadik, A., Tsae, N.B., Rai, S.S., Fissha, Y., Okada, N., and Kawamura, Y. Advancing Iron Ore Grade Estimation: A Comparative Study of Machine Learning and Ordinary Kriging. Minerals, 15(2), 131 (2025). https://doi.org/10.3390/min15020131

[1]*Ныгманова А.С.,
магистр, аға оқытушы, ORCID ID: 0009-0003-3917-2707,
e-mail: a.emls@kbtu.kz
[1]Коробкин В.В.,
г.-м.ғ.к., профессор, ORCID ID: 0000-0002-1562-759X,
e-mail: korobkin_vv@kbtu.kz
[2]Буслов М.М.,
г.-м.ғ.д., профессор, ORCID ID: 0000-0003-0606-2264,
e-mail: buslov@igm.nsc.ru
[1]Чакликов А.Е.,
PhD, ассистент-профессор, ORCID ID: 0000-0001-8316-6599,
e-mail: a.chaklikov@kbtu.kz
[1]Тулемисова Ж.С.,
PhD, қауымдастырылған профессор, ORCID ID: 0000-0003-1803-4535,
e-mail: z.tulemissova@kbtu.kz
[1,3]Койшибаев С.М.,
магистрант, кеңесші геолог, ORCID ID: 0009-0005-6492-4215
e-mail: skoishibayev@srk.kz

[1,3]Қазақстан-Британ техникалық университеті, Алматы қ., Қазақстан
[2]В.С. Соболев атындағы Геология және минералогия институты, Ресей ғылым академиясының Сібір бөлімшесі, Новосібір мемлекеттік университеті, Новосібір қ., Ресей
[3]SRK Consulting, Алматы қ., Қазақстан

ОРТАЛЫҚ ҚАЗАҚСТАННЫҢ СОЛТҮСТІК-БАТЫС БАЛҚАШ ӨҢІРІНДЕГІ ТЕМІР СКАРНДАРЫНЫҢ ҚАЛЫПТАСУЫН БАҚЫЛАЙТЫН ГЕОЛОГИЯЛЫҚ ЖӘНЕ МИНЕРАЛОГИЯЛЫҚ ФАКТОРЛАР

Аңдатпа

Кешенді зерттеу Солтүстік-Батыс Балқаш өңіріндегі темір скарн кенорындарының қалыптасуын анықтайтын негізгі геологиялық және минералогиялық факторларды, Жуантөбе және Қарауылкен сияқты үлгілік кенорындар негізінде айқындады. Геологиялық карталау, минералогиялық және петрографиялық

бақылаулар, геохимиялық деректер мен геофизикалық интерпретациялардың интеграцияланған талдауы скарн түзілуінің магматикалық, құрылымдық және флюидтік факторлармен бақыланатын көпсатылы контактылы-метасоматикалық жүйе екенін көрсетеді. Минералдық қауымдастықтардың таралуы мен кеннің текстуралық-құрылымдық типтеріндегі жүйелі заңдылықтар анықталып, олар флюидтік режимдердің және кен түзілуінің физика-химиялық жағдайларының өзгерістерін бейнелейді. Алынған нәтижелер Солтүстік-Батыс Балқаш өңіріндегі темір скарндарының аймақтық генетикалық моделін нақтылап, жаңа кен нысандарының болжамын жасау және барлау әлеуетін бағалау үшін қолданылуы мүмкін.

Түйін сөздер: скарн кенорындары; магнетитті кендер; контактылы метасоматоз; минералогия; геофизикалық аномалиялар; Солтүстік-Батыс Балқаш өңірі.

[1]*Ныгманова А.С.,
магистр, ст. преподаватель, ORCID ID: 0009-0003-3917-2707,
e-mail: a.emls@kbtu.kz
[1]Коробкин В.В.,
кандидат геолого-минералогических наук, профессор, ORCID ID: 0000-0002-1562-759X,
e-mail: korobkin_vv@kbtu.kz
[2]Буслов М.М.,
доктор геолого-минералогических наук, профессор, ORCID ID: 0000-0003-0606-2264,
e-mail: buslov@igm.nsc.ru
[1]Чакликов А.Е.,
PhD, ассистент-профессор, ORCID ID: 0000-0001-8316-6599,
e-mail: a.chaklikov@kbtu.kz
[1]Тулемисова Ж.С.,
PhD, ассоциированный профессор, ORCID ID: 0000-0003-1803-4535,
e-mail: z.tulemissova@kbtu.kz
[1,3]Койшибаев С.М.,
магистрант, консультант геолог, ORCID ID: 0009-0005-6492-4215
e-mail: skoishibayev@srk.kz

[1,3]Казахстанско-Британский технический университет, г. Алматы, Казахстан
[2]Институт геологии и минералогии им. В.С. Соболева СО РАН, Новосибирский государственный университет, г. Новосибирск, Россия
[3]SRK Consulting, г. Алматы, Казахстан

ГЕОЛОГИЧЕСКИЕ И МИНЕРАЛОГИЧЕСКИЕ ФАКТОРЫ КОНТРОЛЯ ФОРМИРОВАНИЯ ЖЕЛЕЗНЫХ СКАРНОВ В СЕВЕРО-ЗАПАДНОМ ПРИБАЛХАШЬЕ (ЦЕНТРАЛЬНЫЙ КАЗАХСТАН)

Аннотация

Комплексное исследование позволило выявить основные геологические и минералогические факторы, контролирующие формирование железных скарновых месторождений Северо-Западного Прибалхашья на примере репрезентативных объектов, таких как Жуантобе и Караулкен. Интегрированный анализ данных геологического картирования, минералогических и петрографических наблюдений, геохимических исследований и геофизических интерпретаций показывает, что формирование скарнов представляет собой многостадийную контактно-метасоматическую систему, контролируемую магматическими, структурными и флюидными факторами. Установлены закономерности распределения минеральных ассоциаций и текстурно-структурных типов руд, отражающие изменения флюидных режимов и физико-химических условий рудообразования. Полученные результаты уточняют региональную генетическую модель формирования железных скарнов Северо-Западного Прибалхашья и могут быть использованы для прогноза и оценки перспектив новых рудных объектов.

Ключевые слова: скарновые месторождения, магнетитовые руды, контактный метасоматоз, минералогия, геофизические аномалии, Северо-Западное Прибалхашье.